Improved estimation accuracy of the 5-bases-based tomographic method

L. Zambrano, L. Pereira, and A. Delgado*
Instituto Milenio de Investigación en Óptica, Universidad de Concepción, Concepción, Chile
and Facultad de Ciencias Físicas y Matemáticas, Departamento de Física, Universidad de Concepción, Concepción, Chile

(Received 23 May 2019; published 28 August 2019)

It has been recently shown that for quantum systems with dimension $d \geqslant 4$ unknown pure states can be estimated via measurements on five bases only. Here, we study by means of numerical experiments the estimation accuracy of this method as a function of the dimension and the number of independently, identically prepared copies, that is, ensemble size. We show that the accuracy of this method can be greatly improved by modifying the estimation procedure, without increasing the number of measurement outcomes. The present estimation accuracy becomes approximately d times smaller than the best accuracy achievable by tomographic methods for unknown mixed states. We also study the case of pure states affected by a low level of white noise. We show that the modified version of the method is very robust; that is, it remains to a large extent unaffected by the noise and achieves an accuracy similar to the case without noise.

DOI: 10.1103/PhysRevA.100.022340

I. INTRODUCTION

The main aim of quantum tomography (QT) is the accurate, reliable estimation of unknown quantum states. In the field of quantum information, QT has become a standard tool not only for characterizing quantum states but also for assessing and improving the performance of quantum processes, devices, and experimental setups.

Quantum tomographic methods are based on a set of measurements that are informationally complete onto the set of states to be reconstructed, that is, measurements the statistics of which univocally characterizes quantum states, for instance, eigenvectors of generalized Gell-Mann matrices [1,2], mutually unbiased bases [3–9], and symmetric informationally complete positive operator-valued measures [10–15], among many others [16–21]. These measurements are carried out on an ensemble of identically, independently prepared copies of the state to be estimated. The experimentally acquired data are used to estimate probabilities, which are subsequently employed to determine the unknown state. However, finite statistic effects and unavoidable experimental noise lead to operators that fail to be positive semidefinite. In order to provide a physically acceptable state, the data are postprocessed by means of statistical inference methods such as maximum likelihood estimation [22–24] and Bayesian inference [25].

The minimal number of total measurement outcomes required to determine an unknown d-dimensional quantum state is d^2, which is achieved by means of a generalized measurement with d^2 elements [11]. This quadratic scaling constitutes a severe constraint for the experimental and computational feasibility of quantum tomographic methods, which becomes particularly dramatic for multipartite systems [26]. In this case, the scaling is exponential in the number of components. It is possible to reduce the number of measurement outcomes with the help of quantum tomographic methods that employ *a priori* information about the unknown state such as, for instance, purity [27,28], rank [29,30], distance with respect to a previously known state [31], and states with special properties [32]. The case of highly pure states is of particular importance. Quantum information processes and devices, such as quantum computers, prepare and coherently evolve pure states. In the presence of small errors, the density matrix generated will have a dominant eigenvalue and will be close to a pure state. Randomized benchmarking techniques can be employed to certify operation in this regime.

In addition to the total number of measurement outcomes, ensemble size, that is, the total number N of independently, identically prepared copies, is another costly resource in experimental realizations. This is particularly important in the case of higher-dimensional quantum systems, where the higher the dimension becomes the smaller the ensemble size becomes. This has led recently to the study of quantum tomography from the point of view of the achievable estimation accuracy as a function of the ensemble size N and the dimension d and to the search for methods that achieve the highest possible estimation accuracy. For instance, standard quantum tomography achieves an accuracy, quantified through the infidelity, of the orders of $O(1/\sqrt{N})$ and $O(1/N)$ for pure and mixed states, respectively. It is possible to increase the accuracy for the determination of a pure state by means of two-stage adaptive standard quantum tomography [33–36]. This method allows one to achieve a state independent accuracy of $O(1/N)$ at the expense of doubling the total number of measurements and of requiring adaptive measurements.

Quantum Cramér-Rao [37] and Gill-Massar [38,39] inequalities can be employed to determine whether the accuracy of a tomographic method approaches optimality or not. These inequalities allow one to deduce lower bounds for the value of several figures of merit for the tomographic accuracy, such as infidelity, mean-square error, and trace distance. For example,

*aldelgado@udec.cl

two-stage adaptive standard quantum tomography saturates the Gill-Massar lower bound for the infidelity and the mean-square error for $d = 2$ [36]. In higher dimensions, this result does not hold [34].

Here, we study the accuracy achieved by the process of estimating unknown pure states of higher-dimensional quantum systems. This is motivated by the observation that the value of the Gill-Massar lower bound depends on the number of parameters that describe the set of states to be reconstructed. For a fixed ensemble size, unknown pure states can be estimated with a higher accuracy than unknown mixed states. In the particular case of the infidelity, the Gill-Massar lower bound for the estimation of pure states is approximately d^2 times smaller than the lower bound for the estimation of mixed states. Therefore, tomographic methods for pure states might achieve a higher accuracy than tomographic methods for mixed states, with the added benefit of requiring less measurement outcomes.

In the present paper, we conduct a study of a tomographic method specifically designed for unknown pure states [28]. This method is based on the measurement of five bases on any dimension $d \geqslant 4$. This represents a favorable linear scaling for the total number of measurement outcomes with the dimension: a total number of $5d$ projective measurements is required to determine any pure state. We employ the infidelity between the unknown pure state and its estimate as the figure of merit for accuracy [40]. This choice is dictated by the agreement between the infidelity and the Bures distance in the infinitesimal case [41]. Furthermore, the inverse of the infidelity can be identified with the ensemble size required to achieve a prescribed accuracy. Since the five-bases-based quantum tomographic method (5BB-QT) always delivers a pure quantum state as estimate, the infidelity is simply given by the overlap between the unknown state and its estimate. The 5BB-QT method requires projections onto the states of the canonical base. The results of these measurements are subsequently employed to adapt the remaining four bases. The results of the projections onto these four bases are then employed to solve a recursive system of equations, which leads to an estimate of the unknown state. The estimation accuracy of this method can be greatly improved. We introduce three modifications of the 5BB-QT method, each one leading to a better estimation accuracy. These modifications of the 5BB-QT method differ in the procedure employed to generate the estimate of the unknown state. For instance, it is possible to employ the measurement results of the canonical base to increase the estimation accuracy and the system of equations can be suitably modified to reduce the propagation of errors. The present tomographic methods, however, employ the same number and type of measurements as the 5BB-QT method.

Monte Carlo numerical experiments in a wide range of dimensions show that the expected value of the infidelity, over many determination attempts for a fixed unknown pure state, achieved by the best performing modification of the 5BB-QT method, has the scaling $\alpha d^{1.87}/N$, where α depends on the dimension. This scaling is better than the best achievable accuracy by means of a tomographic method for unknown states that does not rely on *a priori* information, which is given by the Gill-Massar lower bound of $(d^2 - 1)(d + 1)/4N$.

We also study the important case of estimating highly pure states. We consider the effect of white noise on the estimation accuracy, which transforms pure states into mixed states. For a purity of 0.98, we show that the original 5BB-QT method stagnates; that is, an increase of the ensemble size beyond a certain limit does not lead to an improvement of the estimation accuracy. However, one of the modified versions of this method achieves the scaling $\alpha d^{1.86}/N^{0.97}$. This is still better than the Gill-Massar lower bound in the inspected ranges of dimension and ensemble size. This result is achieved without increasing the number of measurement outcomes required to characterize the unknown states. Thereby, our results indicate that the 5BB-QT method can be modified in such a way that it makes possible the highly accurate estimation of pure quantum states even in the presence of white noise. This estimation accuracy is d times better than that achievable by tomographic methods for unknown mixed states. Additionally, the estimation accuracy is nearly state independent, and mean and median exhibit very close values, which are contained in a very narrow interquartile range.

This paper is organized as follows. In Sec. II we briefly introduce the 5BB-QT method. In Sec. III, we introduce three variations of the 5BB-QT method that achieve a higher estimation accuracy than the original method. In Sec. IV, we briefly review some results from quantum estimation theory. In Sec. V, by means of a series of Monte Carlo numerical simulations, we analyze the tomographic accuracy achieved by the 5BB-QT method and its variations. In Sec. VI, we study the impact of white noise on the four tomographic methods. In Sec. VII we summarize, comment on possible experimental realizations, and conclude.

II. FIVE-BASES-BASED QUANTUM TOMOGRAPHIC METHOD

An arbitrary pure state $|\psi\rangle$ of a d-dimensional quantum system is given by the linear combination

$$|\psi\rangle = \sum_{i=0}^{d-1} |c_i| e^{i\phi_i} |i\rangle, \tag{1}$$

where $\mathcal{B}_0 = \{|i\rangle\}$ with $i = 0, \ldots, d-1$ is an arbitrary base of the relevant Hilbert space. This state is completely specified by the values of $2d - 2$ real parameters: $d - 1$ amplitudes $|c_i|$ and $d - 1$ phases ϕ_i.

Let us now consider the polarization identity (for complex numbers) for two consecutive probability amplitudes c_k and c_{k+1}, that is,

$$\begin{aligned} c_k c_{k+1}^* = \tfrac{1}{4}(&|c_k + c_{k+1}|^2 - |c_k - c_{k+1}|^2 \\ &- i|c_k + ic_{k+1}|^2 + i|c_k - ic_{k+1}|^2), \end{aligned} \tag{2}$$

where $|\cdot|$ is the absolute value. The terms entering on the right-hand side of Eq. (2) are proportional to the probability of projecting the unknown state $|\psi\rangle$ onto the non-normalized states $|k\rangle \pm |k+1\rangle$ and $|k\rangle \pm i|k+1\rangle$, respectively. This suggests that unknown pure states can be reconstructed via the iterative application of Eq. (2) on consecutive probability amplitudes. The total set of states required by this procedure to reconstruct any pure state in dimension d can be sorted in five orthonormal bases [28]. These are given by $\mathcal{B}_0$ together

with the four additional bases

$$\mathcal{B}_1 = \left\{ |\varphi_\pm^\nu\rangle_1 = \frac{1}{\sqrt{2}}(|2\nu\rangle \pm |2\nu+1\rangle) \right\},$$
$$\mathcal{B}_2 = \left\{ |\tilde{\varphi}_\pm^\nu\rangle_2 = \frac{1}{\sqrt{2}}(|2\nu\rangle \pm i|2\nu+1\rangle) \right\},$$
$$\mathcal{B}_3 = \left\{ |\varphi_\pm^\nu\rangle_3 = \frac{1}{\sqrt{2}}(|2\nu+1\rangle \pm |2\nu+2\rangle) \right\},$$
$$\mathcal{B}_4 = \left\{ |\tilde{\varphi}_\pm^\nu\rangle_4 = \frac{1}{\sqrt{2}}(|2\nu+1\rangle \pm i|2\nu+2\rangle) \right\}, \quad (3)$$

where $\nu \in [0, (d-2)/2]$. Operations with labels are carried out modulo d. In the case of odd dimensions, the integer part of $(d-2)/2$ is considered and every basis is completed with the state $|d\rangle$.

Defining coefficient $p_\pm^{(k)}$ with k even (odd) as the transition probability from the unknown pure state $|\psi\rangle$ to the state $|\varphi_\pm^k\rangle$ in basis $\mathcal{B}_1$ ($\mathcal{B}_3$) and $\tilde{p}_\pm^{(k)}$ with k even (odd) as the transition probability from the unknown state to the state $|\varphi_\pm^k\rangle$ in basis $\mathcal{B}_2$ ($\mathcal{B}_4$), the 5BB-QT method can be defined by the system of equations

$$2c_k c_{k+1}^* = \Lambda_k, \quad (4)$$

with

$$\Lambda_k = (p_+^{(k)} - p_-^{(k)}) + i(\tilde{p}_+^{(k)} - \tilde{p}_-^{(k)}). \quad (5)$$

The solutions of Eq. (4), that is, the coefficients c_k entering in the unknown pure state $|\psi\rangle$, can be recursively calculated as

$$c_k = \begin{cases} c_0 \prod_{j=0}^{k/2-1} \frac{\Lambda_{2j+1}^*}{\Lambda_{2j}}, & k > 0 \text{ even}, \\ \frac{\Lambda_0^*}{2c_0} \prod_{j=0}^{(k-3)/2} \frac{\Lambda_{2j+2}^*}{\Lambda_{2j+1}}, & k > 1 \text{ odd}, \end{cases} \quad (6)$$

where $c_1 = \Lambda_0^*/2c_0$ and c_0 is obtained from the normalization condition $\sum_k |c_k|^2 = 1$.

Let us note that bases $\mathcal{B}_i$ with $i = 1, \ldots, 4$ allow one to determine any pure state up to a null-measure set, which corresponds to the statistically unlikely $(d-2)$-dimensional manifold of states with two or more nonconsecutive vanishing amplitudes. Base $\mathcal{B}_0$ is employed to detect whether a state belongs to this manifold or not. If the state belongs to the manifold, then it can be reconstructed with the remaining four bases but adapted to a known lower-dimensional subspace.

III. MODIFICATIONS OF THE FIVE-BASES-BASED QUANTUM TOMOGRAPHIC METHOD

The 5BB-QT method employs the base $\mathcal{B}_0$ to decide whether a state can be reconstructed with bases $\mathcal{B}_i$ or with an adaptation of the bases $\mathcal{B}_i$ to a lower-dimensional subspace. Thereby, unknown states are always estimated by means of projections on bases $\mathcal{B}_i$, or its adapted version, and the information about the probability amplitudes of the unknown state provided by the projections on the base $\mathcal{B}_0$ remains unused.

The estimate of the unknown state is given by the solution Eq. (6) of the equation system Eq. (4). The solution Eq. (6) is of iterative nature; that is, to estimate the coefficient c_k we need the information provided by the measurements on bases $\mathcal{B}_i$ and, in addition, the value of all coefficients $c_{k'}$ with $k' < k$. Thereby, estimation errors in the probabilities $p_\pm^{(k)}$ and $\tilde{p}_\pm^{(k)}$ are propagated across the coefficients. Thus, the 5BB-QT method might lead to estimates of low accuracy.

There are, however, modifications of the estimation procedure employed by the 5BB-QT method that can help to increase significantly the estimation accuracy. For instance, the base $\mathcal{B}_0$ allows for an easy estimation of the amplitudes $|c_k|$, where each one is estimated independently. Thus, we can estimate the complex phases $e^{i\phi_k}$ by means of the solution Eq. (6) and combine them with the estimates of the amplitudes $|c_k|$ provided by the base $\mathcal{B}_0$. This method is referred to as the corrected 5BB-QT (C5BB-QT) method. Since we only modify the estimation procedure, the C5BB-QT and 5BB-QT methods employ the same measurements.

We can also modify the 5BB-QT method to reduce the impact of small amplitudes in the accuracy of the estimation of the complex phases, which in turn can improve the estimation accuracy of the unknown states. First, we proceed to measure the diagonal basis $\mathcal{B}_0$, which will give us an idea of the size of each of the amplitudes $|c_i|$. Then, we apply an operator U_p that permutes the probability amplitudes of the state, in such a way that the state

$$|\psi_p\rangle = U_p|\psi\rangle = \sum_{i=0}^{d-1} c_i'|i\rangle \quad (7)$$

has the amplitudes in decreasing order, that is, $|c_0'| \geqslant |c_1'| \geqslant \ldots \geqslant |c_{d-1}'|$. Finally, we apply the 5BB-QT method to this new state, which will lead to an estimate $|\psi_p'\rangle$. To obtain the estimate $|\psi'\rangle$, we only need to apply the inverse transformation $U_p^\dagger$. This method will be referred to as the improved 5BB-QT method (I5BB-QT).

In this modification of the 5BB-QT method, the total number of measurements is still $5d$, since the adaptation is made after measuring the diagonal base $\mathcal{B}_0$, which provides information about the modulus of the coefficients. The operator U_p only permutes the coefficients, and due to this it does not erase the information obtained before the adaptation. We can thus now combine both modifications, that is, the direct estimation of the amplitudes $|c_k|$ via the base $\mathcal{B}_0$ and the use of the operator U_p, to increase the accuracy in the estimation of the complex phases $e^{i\phi_k}$. This will be referred to as the improved corrected 5BB-QT method (IC5BB-QT).

As we will show in the next sections, the modification of the 5BB-QT method leads to a significant increase in the estimation accuracy, even in the case of estimating pure states affected by white noise.

IV. QUANTUM ESTIMATION THEORY

In order to study the accuracy of the 5BB-QT method and its variation, we employ Fisher's theory of statistical estimation. This leads to inequalities for the estimation uncertainty of the parameters of a quantum state, which are obtained by means of a measurement strategy. The relevant inequalities are the Cramér-Rao inequality $\mathcal{C} \leqslant \mathcal{I}^{-1}$ [37], the quantum Cramér-Rao inequality $\mathcal{C} \leqslant \mathcal{J}^{-1}$ [37], and the Gill-Massar inequality $\mathrm{Tr}(\mathcal{I}\mathcal{J}^{-1}) \leqslant d-1$ [38], where $\mathcal{C}$ is the covariance matrix, $\mathcal{I}$ is the classical Fisher information matrix, and $\mathcal{J}$ is the quantum Fisher information matrix. These inequalities consider the impact of a finite ensemble size on the estimation

uncertainty and allow one to establish fundamental lower bounds for several error measures, for instance, infidelity or mean-square error. These bounds represent the ultimate accuracy permitted by the laws of quantum mechanics. However, Fisher's theory does not give hints about which measurements allow one to attain the bounds: finding these measurements is a contemporary challenging problem, especially in the multiparameter case, which is precisely the context of quantum tomography.

We employ the infidelity as figure of merit [40]. This is a simple and well-motivated distance between two quantum states ρ and $\tilde{\rho}$ that is defined by

$$I(\rho, \tilde{\rho}) = 1 - \mathrm{Tr}(\sqrt{\sqrt{\rho}\tilde{\rho}\sqrt{\rho}})^2. \tag{8}$$

In particular, if the considered states are pure, that is, $\rho = |\psi\rangle\langle\psi|$ and $\tilde{\rho} = |\tilde{\psi}\rangle\langle\tilde{\psi}|$, the infidelity is reduced to the overlap between states $I(|\psi\rangle, |\tilde{\psi}\rangle) = 1 - |\langle\psi|\tilde{\psi}\rangle|^2$. The infidelity has two important properties that motivate its use: for infinitesimally close states, it agrees with the Bures metric [41] and its inverse can be identified with the sample size required to reach a prescribed accuracy [33]. Depending on the measurement strategy and the number of independent parameters, different lower bounds for the mean infidelity $\bar{I}$ are known. The mean infidelity is the expected value of the infidelity with respect to all possible estimates $\tilde{\rho}$ of a state ρ, that is,

$$\bar{I}(\rho) = \int I(\rho, \tilde{\rho}) f(\tilde{\rho}) d\tilde{\rho}, \tag{9}$$

where $f(\tilde{\rho})$ is the probability density function of obtaining the estimate $\tilde{\rho}$.

For the estimation of pure states, which have $2(d-1)$ independent parameters, the ultimate accuracy is given by the Gill-Massar bound [39]

$$I_{\mathrm{GM}}^{(\mathrm{pure})} = (d-1)/N. \tag{10}$$

For mixed states, which have $d^2 - 1$ independent parameters, and when the measurement strategy is restricted to individual measurements, that is, measurements on single members of the ensemble, the ultimate limit is the Gill-Massar bound [39]:

$$I_{\mathrm{GM}}^{(\mathrm{mixed})} = (d^2-1)(d+1)/4N. \tag{11}$$

If collective measurements, that is, measurements that are carried out on several members of the ensemble, are allowed, the ultimate limit is the quantum Cramér-Rao bound $I_{\mathrm{CR}} = (d^2 - 1)/4N$. Thereby, the accuracy achieved by a tomographic method can be studied by comparing its mean infidelity $\bar{I}$ with the corresponding bound.

In general, the behavior of the mean infidelity as function of the ensemble size can be fitted with the monomial $\bar{I}(\alpha, \beta) = \alpha N^{\beta}$, so the tomographic protocols are characterized by its proportionality constant α and its scaling β. Let us note that α and β might be functions of the dimension d. For instance, it is known that standard quantum tomography for a single qubit delivers a mean infidelity for pure states that scales as $O(1/\sqrt{N})$ while for mixed states it scales as $O(1/N)$. Two-stage adaptive standard tomography achieves an infidelity that scales as $O(1/N)$ for all quantum states [33,34]. In the particular case of $d = 2$, two-stage adaptive standard quantum tomography saturates the Gill-Massar bound $I_{\mathrm{GM}}^{(\mathrm{mixed})}$ [39]. This, however, does not hold for $d > 2$.

Clearly, it is possible to determine pure states by means of tomographic methods designed to reconstruct any quantum state. These, however, are at disadvantage with respect to tomographic methods specifically designed to determine pure states, because the bound $I_{\mathrm{GM}}^{(\mathrm{pure})}$ for pure states is lower than the bound $I_{\mathrm{GM}}^{(\mathrm{mixed})}$ for density matrices. For large d, the difference between both bounds scales quadratically with the dimension. Therefore, tomographic methods specifically designed to determine pure states have the potential to achieve a higher accuracy than the best tomographic method for density matrices. Furthermore, tomographic methods for pure states require less measurement outcomes than methods for mixed states. Moreover, *a priori* information, such as purity, range, or distance with respect to another state [31], reduces the number of parameters of the states, decreases the value of the bound, and, therefore, helps to formulate tomographic methods with a higher accuracy for specific families of quantum states.

V. NUMERICAL SIMULATIONS

In this section we study the accuracy of the 5BB-QT, C5BB-QT, I5BB-QT, and CI5BB-QT methods. In particular, we analyze the dependence of the mean infidelity $\bar{I}(|\psi\rangle)$ with respect to the ensemble size N and the dimension d of the Hilbert space.

In order to estimate the value of the mean infidelity $\bar{I}(|\psi\rangle)$ we resort to Monte Carlo simulations. For a given dimension d, we generate a set Ω_d composed of 10^2 pure quantum states that are drawn from a uniform distribution on the Hilbert space. The determination of each state $|\psi_i\rangle \in \Omega_d$ $(i = 1, \ldots, 10^2)$ by means of each one of the tomographic methods is simulated 100 times considering a finite ensemble size N. This procedure generates for each state $|\psi_i\rangle$ 100 estimates $|\tilde{\psi}_j\rangle$ and 100 values of the infidelity $I(|\psi_i\rangle, |\tilde{\psi}_j\rangle)$ $(j = 1, \ldots, 100)$.

Figure 1 displays, in logarithmic scale for both axes, the behavior of the mean and the median of the infidelity $\bar{I}(|\psi_i\rangle)$ as a function of N obtained by means of the 5BB-QT (solid brown dots), C5BB-QT (solid red stars), I5BB-QT (solid blue squares), and CI5BB-QT (light blue crosses) methods for four randomly selected states $|\psi_i\rangle$ in Ω_d with $d = 4$. The mean infidelity $\bar{I}(|\psi_i\rangle)$ is estimated according to the equation

$$\bar{I}(|\psi_i\rangle) = 10^{-2} \sum_{j=1}^{100} I(|\psi_i\rangle, |\tilde{\psi}_j\rangle). \tag{12}$$

This quantity can be properly compared with the relevant bounds provided by the Gill-Massar inequality. As is apparent from the left column of Fig. 1, the CI5BB-QT and the I5BB-QT methods reach in all four cases infidelities that are almost indistinguishable. These methods also generate consistently the lowest infidelities, or the highest estimation accuracies, in the four inspected cases. The 5BB-QT and the C5BB-QT methods provide mixed results. For a single state, which is illustrated in the second row in Fig. 1, the 5BB-QT and the C5BB-QT methods achieve infidelities that are comparable to the ones achieved by the I5BB-QT and the CI5BB-QT

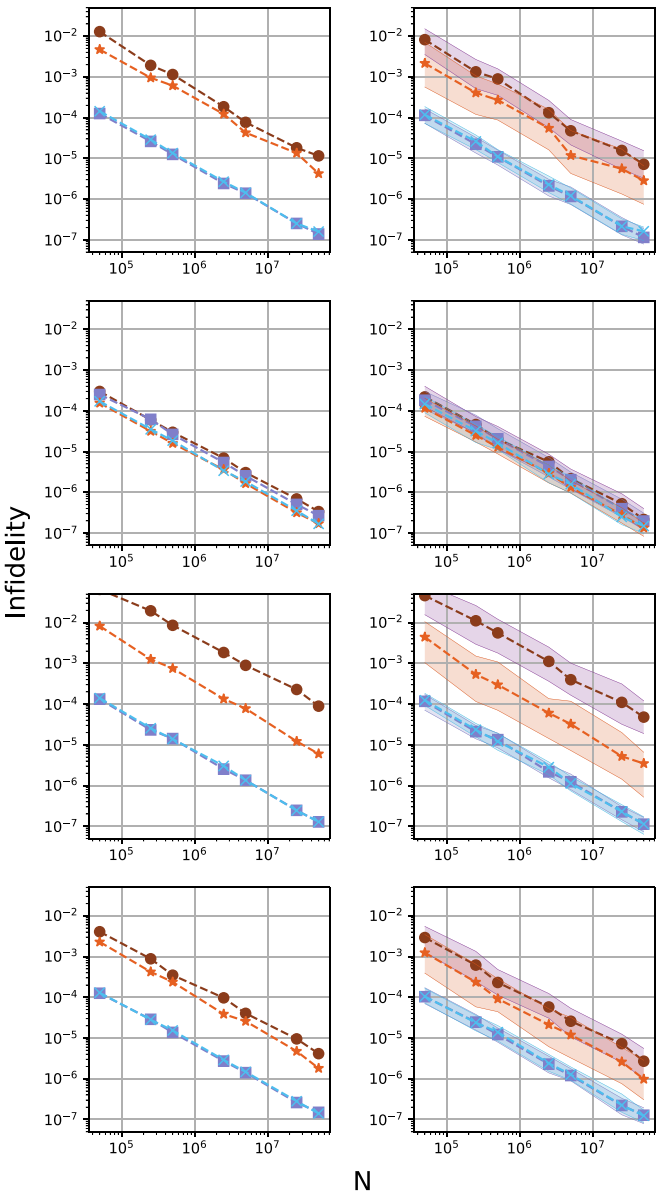

FIG. 1. The left (right) column shows the mean (median) infidelity $\bar{I}(|\psi\rangle)$, as a function of the ensemble size N, obtained via the 5BB-QT (solid brown dots), C5BB-QT (solid red stars), I5BB-QT (solid blue squares), and CI5BB-QT (light blue crosses) methods for four randomly chosen states in $d = 4$. Shaded areas represent the corresponding interquartile range.

methods. For the remaining three states (first, third, and fourth rows in Fig. 1), the infidelities achieved by the 5BB-QT and the C5BB-QT methods are approximately two orders of magnitude higher than the ones achieved by the I5BB-QT and the CI5BB-QT methods.

A similar result is illustrated in the right column of Fig. 1, where the median of the infidelity $\bar{I}(|\psi_i\rangle)$ is displayed together with the respective interquartile range (shaded areas). All estimation methods generate similar values for the mean and median infidelity, which is an indication of a symmetric probability distribution $f(\tilde{\rho})$. However, states where the 5BB-QT and the C5BB-QT methods provide a higher infidelity are characterized by a wider interquartile range, which indicates a larger variability in comparison to the I5BB-QT and CI5BB-QT methods. These two methods lead to similar interquartile ranges for the four randomly selected states.

An additional feature of Fig. 1 is that mean and median infidelity exhibit a linear dependence with the ensemble size N. This suggests approximating $\bar{I}(|\psi_i\rangle)$ by the monomial αN^{β}, where coefficients α and β might depend on the dimension d of the underlying Hilbert space.

Figure 2 displays, in logarithmic scale for both axes, the average $\langle\bar{I}\rangle$ (solid dots) of the mean infidelity $\bar{I}(|\psi_i\rangle)$, generated by each one of the estimation methods, over the set Ω_d as a function of the ensemble size N for dimension $d = 4, 8, 16, 32,$ and 64, from bottom to top. This average is estimated as the mean of $\bar{I}(|\psi_i\rangle)$ on Ω_d, that is,

$$\langle\bar{I}\rangle = 10^{-2}\sum_{i=1}^{100}\bar{I}(|\psi_i\rangle). \tag{13}$$

Figure 2 also displays other relevant central tendency indicators such as median (solid stars) and interquartile range (shaded areas) for each dimension.

In all four subplots in Fig. 2, the mean and median of $\bar{I}(|\psi_i\rangle)$ in Ω_d exhibit a linear dependence with the ensemble size, which is different for each estimation method. Figure 2(a) displays the average accuracy generated by the 5BB-QT method, which is characterized by a median that reaches a lower value than the average. This shows that the 5BB-QT method is characterized by a state dependent estimation accuracy. The average of $\bar{I}(|\psi_i\rangle)$ is located approximately at the upper border of the interquartile range, which indicates that 25% of the states in Ω_d are estimated with an accuracy lower than the average. The resting states are estimated with a better accuracy. This occurs for all inspected dimensions. Figure 2(b) shows the average accuracy that is generated by means of the C5BB-QT method. As in the previous case, the median reaches a lower value than the average. However, the average tends to be located beyond the interquartile range, which indicates the existence of estimation attempts characterized by small estimation accuracies and a variability wider than the one exhibited by the 5BB-QT method. Nevertheless, the average infidelity achieved by the C5BB-QT method is approximately 0.5 times smaller than the one achieved by the 5BB-QT method. The situation in Figs. 2(c) and 2(d) is radically different. Here, the I5BB-QT and CI5BB-QT methods exhibit an average and a median of $\bar{I}(|\psi_i\rangle)$ that are indistinguishable from each other. Furthermore, the shaded areas depicting the interquartile range are very narrow fringes, when compared to the cases of the 5BB-QT and C5BB-QT methods in Figs. 2(a) and 2(b), respectively. This indicates that the I5BB-QT and CI5BB-QT methods estimate all states in Ω_d with an accuracy that is approximately independent of the state to be estimated. This accuracy is then well represented by the average $\langle\bar{I}\rangle$, which exhibits a lineal behavior with the ensemble size. The CI5BB-QT method achieves an average infidelity that is approximately 0.5 times smaller than the one achieved by the I5BB-QT method. Thereby, the estimation provided by the CI5BB-QT method achieves the highest accuracy among the four estimation methods. This can be one order of magnitude better than the one exhibited by the 5BB-QT method. In higher dimensions, the

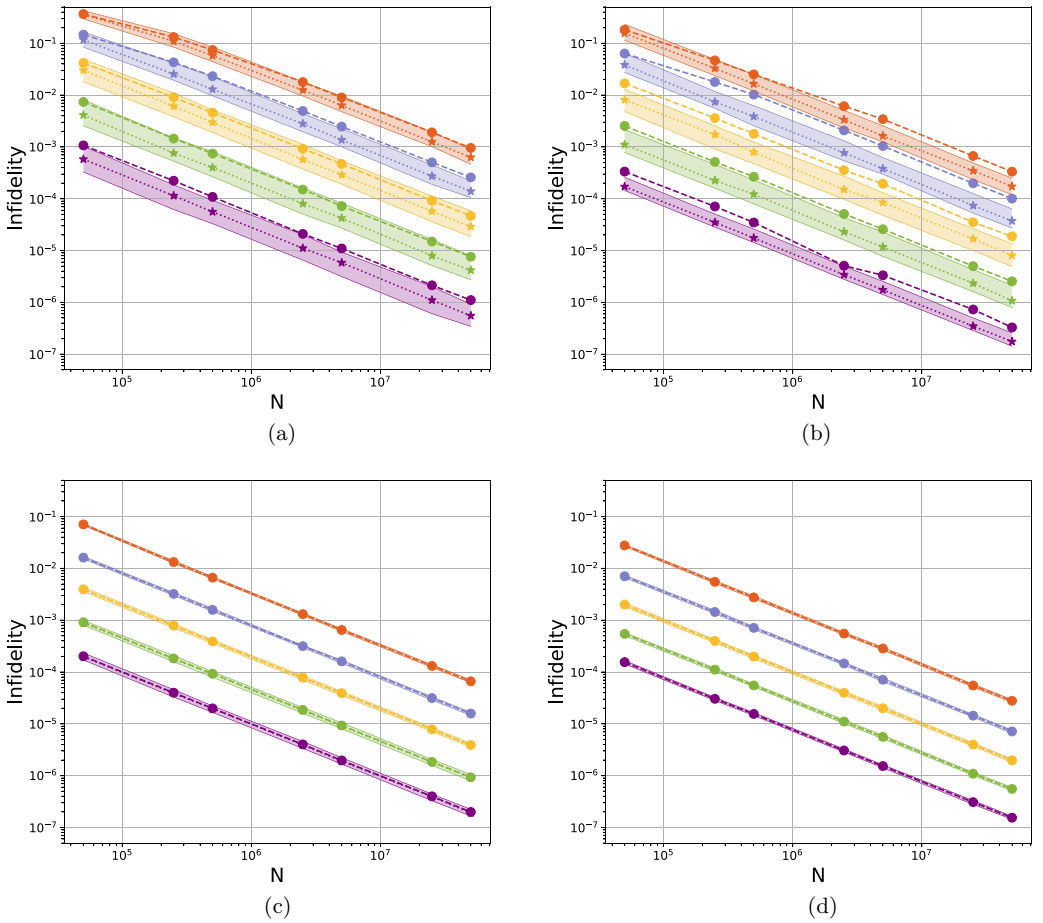

FIG. 2. Mean (solid dots) and median (solid stars) of $\bar{I}$ on Ω_d as a function of ensemble size N, for dimension $d = 4$ (purple), 8 (green), 16 (yellow), 32 (blue), and 64 (red), obtained by means of the four different estimation methods: (a) 5BB-QT method, (b) C5BB-QT method, (c) I5BB-QT method, and (d) CI5BB-QT method. Shaded areas represent interquartile range.

CI5BB-QT method performs even better. For instance, for $d = 64$ the 5BB-QT method reaches an average infidelity of 10^{-3} while the CI5BB-QT method achieves an average infidelity of 3×10^{-5}.

The estimation accuracy also depends on the dimension d that characterizes the system to be estimated. This is studied in Fig. 3, which illustrates the average (solid dots) and the median (solid stars) of $\bar{I}(|\psi_i\rangle)$ over Ω_d, obtained by the four estimation methods, as a function of d for ensemble sizes $N = 5 \times 10^4, 10^5, 5 \times 10^5, 10^6, 5 \times 10^6$, and 10^7 (from top to bottom). As the dimension increases, the average and the median decrease for a fixed ensemble size. The 5BB-QT and C5BB-QT methods [Figs. 3(a) and 3(b), respectively] show an average located above the median for all inspected dimensions and ensemble sizes. In this case, however, average and median do not exhibit a liner behavior with the dimension d. Thereby, the accuracy of these two methods clearly departs from the Gill-Massar lower bounds $I_{\mathrm{GM}}^{\mathrm{pure}}$ and $I_{\mathrm{GM}}^{\mathrm{mixed}}$, which exhibit a lineal behavior with the dimension.

The situation is different in the case of the I5BB-QT and CI5BB-QT methods, which is illustrated in Figs. 3(c) and 3(d), respectively. As is apparent from these figures, the I5BB-QT and CI5BB-QT methods are characterized by an accuracy located approximately one order of magnitude below the one achieved by the 5BB-QT method. However, unlike the 5BB-QT method and within the set of inspected dimensions, the I5BB-QT and CI5BB-QT methods exhibit a linear behavior of the average and the median of $\bar{I}(|\psi_i\rangle)$, akin to the Gill-Massar lower bounds for pure and mixed states. This suggests that the average infidelity of the I5BB-QT and CI5BB-QT methods can be approximated by the monomial $\alpha d^{\gamma} N^{-\beta}$.

In order to obtain the values of the coefficients α, β, and γ for the best performing CI5BB-QT method, we approximate the mean infidelity $\bar{I}(|\psi_i\rangle)$ by means of the function

$$\log_{10}[\bar{I}(|\psi_i\rangle)] = \log_{10}(\alpha) - \beta \log_{10}(N) + \gamma \log_{10}(d), \quad (14)$$

which depends linearly on the logarithms of the ensemble size N and of the dimension d. For a fixed value of dimension d, we obtain 100 values of β, one for each state in Ω_d to be estimated. The mean value $\bar{\beta}$ of β in Ω_d is indicated in Table I, together with the standard deviation, as a function of the dimension. As is apparent from Table I, $\bar{\beta}$ turns out to be independent of the dimension and well represented by the choice $\bar{\beta} = 1$. Similarly, Table I exhibits the value of the mean value $\bar{\gamma}$ of γ in Ω_d as a function of the ensemble size N. This mean value is also independent of N and well represented by the value $\gamma = 1.87$. Thereby, we can approximate the average

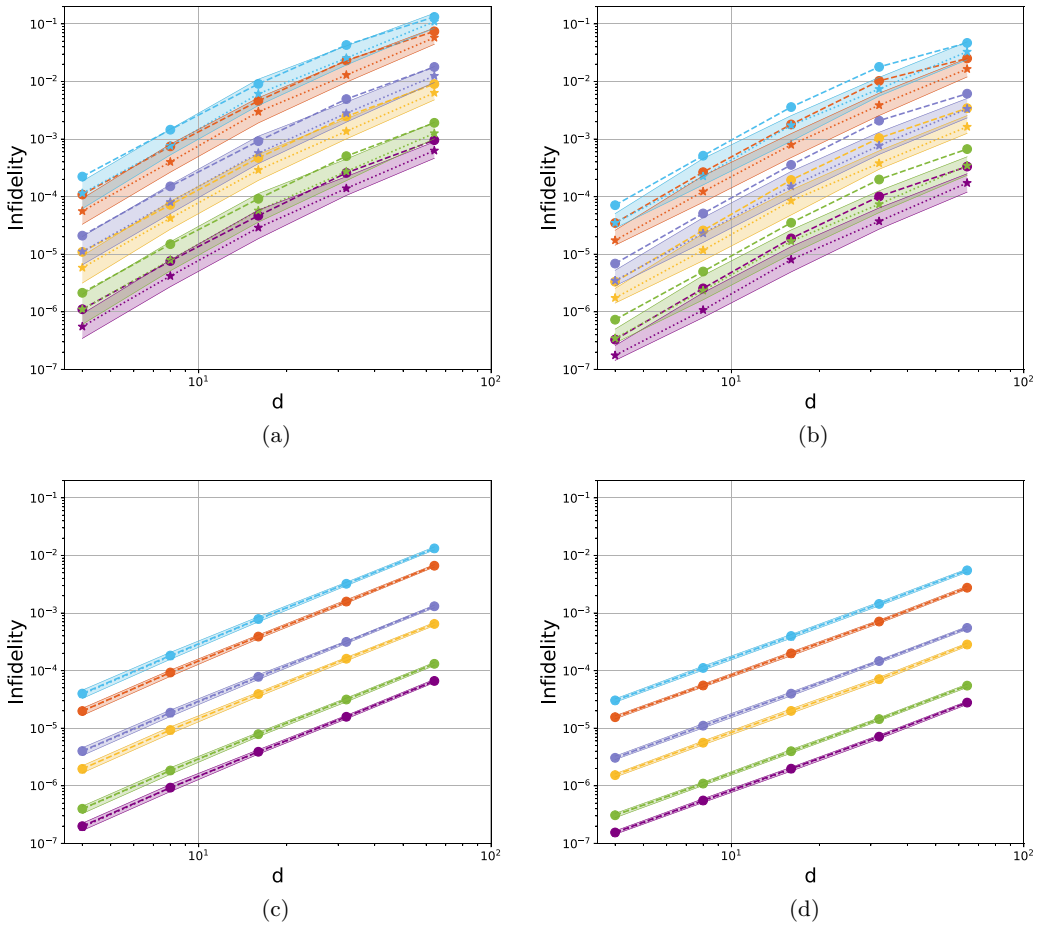

FIG. 3. Mean (solid dots) and median (solid stars) of $\bar{I}$ on Ω_d as a function of the dimension d, obtained by means of the four different estimation methods, for ensemble size $N = 5 \times 10^4$ (purple), 10^5 (green), 5×10^5 (yellow), 10^6 (blue), 5×10^6 (red), and 10^7 (lightblue): (a) 5BB-QT method, (b) C5BB-QT method, (c) I5BB-QT method, and (d) CI5BB-QT method. Shaded areas represent interquartile range.

infidelity achieved by the CI5BB-QT method as

$$\langle \bar{I} \rangle \approx \alpha \frac{d^{1.87}}{N}, \tag{15}$$

where the values of α as a function of the dimension are displayed in Table I. Since the distribution of the mean infidelity $\bar{I}(|\psi_i\rangle)$ is characterized by a very narrow interquartile range, we can perform a further approximation, that is,

$$\bar{I}(|\psi_i\rangle) \approx \alpha \frac{d^{1.87}}{N}, \tag{16}$$

TABLE I. Mean values and standard deviations of the coefficients α, β, and γ entering in the lineal fit of the mean infidelity, Eq. (14), generated by the CI5BB-QT method.

d	$\bar{\alpha} \pm \Delta_\alpha$	$\bar{\beta} \pm \Delta_\beta$	N	$\bar{\gamma} \pm \Delta_\gamma$
4	1.73 ± 0.01	0.99 ± 0.01	10^7	1.87 ± 0.05
8	1.76 ± 0.01	1.00 ± 0.01	5×10^6	1.87 ± 0.04
16	1.79 ± 0.005	1.00 ± 0.02	10^6	1.87 ± 0.04
32	1.81 ± 0.02	1.00 ± 0.02	5×10^5	1.87 ± 0.05
64	1.71 ± 0.02	0.99 ± 0.02	10^5	1.86 ± 0.04
			5×10^4	1.87 ± 0.05

for all $|\psi_i\rangle$ in Ω_d. The previous result can be appropriately compared to the Gill-Massar lower bound for pure and mixed states. The mean infidelity generated by the CI5BB-QT method, Eq. (16), compares favorably with the lower bound $I_{\mathrm{GM}}^{\mathrm{mixed}}$, since the latter behaves, for d large, as $I_{\mathrm{GM}}^{\mathrm{mixed}} \approx d^3/4N$. For all inspected dimensions and states, the CI5BB-QT method achieves a mean infidelity that is much lower than $I_{\mathrm{GM}}^{\mathrm{mixed}}$.

Thereby, the CI5BB-QT method leads to an estimation accuracy for unknown pure states that surpasses the best possible estimation accuracy for unknown mixed states, with the added benefit of requiring many fewer measurement outcomes. The CI5BB-QT method exhibits another interesting feature; namely, it produces a mean and a median that are nearly indistinguishable and contained in a very narrow interquartile range.

As we shall see in the next section, the advantages obtained via the CI5BB-QT method hold even in the presence of white noise.

VI. PERFORMANCE OF THE 5BB-QT METHOD AND ITS MODIFICATIONS UNDER NOISE

The tomographic methods here studied have been designed to estimate pure states. Nevertheless, experimentally

generated states are mixed. It is possible, however, to experimentally generate highly pure states. Here, we study the accuracy of the 5BB-QT, C5BB-QT, I5BB-QT, and CI5BB-QT methods in this regime. In particular, we will assume that the states to be reconstructed are affected by white noise.

Unknown pure states $|\psi\rangle$ affected by white noise are transformed into mixed states of the form

$$\rho = (1-\lambda)|\psi\rangle\langle\psi| + \frac{\lambda}{d}\mathbb{I}, \tag{17}$$

where $\mathbb{I}$ is the identity operator and λ is the mixing parameter. The purity $\mathrm{Tr}(\rho^2)$ of this state and the parameter $\lambda \in [0, 1]$ are related by the expression

$$\lambda = 1 - \sqrt{\frac{\mathrm{Tr}(\rho^2) - 1/d}{1 - 1/d}}. \tag{18}$$

Since the initially unknown pure state $|\psi\rangle$ becomes a mixed state ρ, an estimate of $|\psi\rangle$ can be obtained by estimating ρ via a quantum tomographic method for unknown mixed states and the error model for white noise. This procedure increases the number of measurement outcomes and decreases the achievable estimation accuracy. However, as we will show, it is possible to employ the CI5BB-QT method to obtain an estimate of $|\psi\rangle$ in the presence of white noise without a significant decrease in the estimation accuracy; that is, the estimation procedure reaches an accuracy that is very close to the case without white noise.

Let us now consider the impact of the white noise on the 5BB-QT method defined by Eqs. (4)–(6). The transition probabilities p'_k affected by the white noise are related to the transition probabilities p_k of the unknown state $|\psi\rangle$ by the relation

$$p'_k = (1-\lambda)p_k + \frac{\lambda}{d}, \tag{19}$$

which leads to the noisy Λ'_k given by

$$\Lambda'_k = (1-\lambda)\Lambda_k. \tag{20}$$

Thereby, the system of equations (4) has now the solution

$$c'_k = \begin{cases} c'_0 \prod_{j=0}^{k/2-1} \frac{\Lambda'^*_{2j+1}}{\Lambda'_{2j}} = \frac{c'_0}{c_0} c_k, & k > 0 \text{ even}, \\ \frac{\Lambda'^*_0}{2c'_0} \prod_{j=0}^{(k-3)/2} \frac{\Lambda'^*_{2j+2}}{\Lambda'_{2j+1}} = (1-\lambda)\frac{c_0}{c'_0} c_k, & k > 1 \text{ odd}, \end{cases} \tag{21}$$

where $c'_0 = \sqrt{p'_0}$ and $c'_1 = \Lambda'^*_0/2c'_0 = (1-\lambda)c_0 c_1/c'_0$. Since the coefficients c'_0, c_0, and $(1-\lambda)$ are positive, the probability amplitudes c'_k and c_k have the same complex phase. Thus, the 5BB-QT method in the presence of white noise provides an estimate $|\psi'\rangle$ of $|\psi\rangle = \sum_k c_k e^{i\phi_k}|k\rangle$ given by

$$|\psi'\rangle = \frac{\sqrt{(1-\lambda)c_0^2 + \frac{\lambda}{d}}}{c_0} \sum_{k\geqslant 0 \text{ even}} |c_k| e^{i\phi_k}|k\rangle + \frac{(1-\lambda)c_0}{\sqrt{(1-\lambda)c_0^2 + \frac{\lambda}{d}}} \sum_{k\geqslant 1 \text{ odd}} |c_k| e^{i\phi_k}|k\rangle, \tag{22}$$

or equivalently

$$|\psi'\rangle = \frac{\sqrt{(1-\lambda)c_0^2 + \frac{\lambda}{d}}}{c_0}|\psi\rangle - \frac{\lambda}{d c_0 \sqrt{(1-\lambda)c_0^2 + \frac{\lambda}{d}}} \sum_{k\geqslant 1 \text{ odd}} |c_k| e^{i\phi_k}|k\rangle. \tag{23}$$

Calculating the inner product between $|\psi\rangle$ and $|\psi'\rangle$, we have

$$\langle\psi|\psi'\rangle = \frac{\sqrt{(1-\lambda)c_0^2 + \frac{\lambda}{d}}}{c_0} - \frac{\lambda}{d c_0 \sqrt{(1-\lambda)c_0^2 + \frac{\lambda}{d}}} \sum_{k\geqslant 1 \text{ odd}} |c_k|^2. \tag{24}$$

Taking the square of Eq. (24), we obtain

$$|\langle\psi|\psi\rangle|^2 = 1 - \lambda + \frac{\lambda}{d c_0^2}\left(1 - 2\sum_{k\geqslant 1 \text{ odd}} |c_k|^2\right) + \frac{\lambda^2}{d^2 c_0^2\left[(1-\lambda)c_0^2 + \frac{\lambda}{d}\right]}\left(\sum_{k\geqslant 1 \text{ odd}} |c_k|^2\right)^2. \tag{25}$$

Thereby, the infidelity between $|\psi\rangle$ and $|\psi'\rangle$ is given by the expression

$$I(|\psi\rangle, |\psi'\rangle) = \lambda - \frac{\lambda}{d c_0^2}\left(1 - 2\sum_{k\geqslant 1 \text{ odd}} |c_k|^2\right) - \frac{\lambda^2}{d^2 c_0^2\left[(1-\lambda)c_0^2 + \frac{\lambda}{d}\right]}\left(\sum_{k\geqslant 1 \text{ odd}} |c_k|^2\right)^2, \tag{26}$$

which is bigger than zero for $\lambda \neq 0$. Thus, the estimate $|\psi'\rangle$ provided by the 5BB-QT method will be different from the original unknown state $|\psi\rangle$, as long as $\lambda \neq 0$, which is a great disadvantage of the protocol.

Figure 4 displays the mean (solid dots) and the median (solid stars) of $\bar{I}(|\psi_i\rangle)$ onto Ω_d as a function of the ensemble size N, obtained by means of the four estimation methods, with a constant purity of 0.98. Figure 4(a) shows the accuracy achieved by the 5BB-QT method. As is apparent from this figure, the average $\langle\bar{I}\rangle$ becomes a constant independent of the ensemble size N for all dimensions. Thereby, an increase in the ensemble size does not lead to an increase in the estimation accuracy and, consequently, the 5BB-QT method stagnates. The average infidelity $\langle\bar{I}\rangle$ tends to localize asymptotically around $\langle\bar{I}\rangle \approx 10^{-3}$ for all dimensions. This conveys a severe loss of accuracy with respect to the case of unitary purity [see Fig. 2(a)]. For instance, in the particular case of $d = 4$, the average infidelity is increased from 10^{-6} to 10^{-3} for $N = 5 \times 10^{-7}$. Figure 4(a) also exhibits an increase of several orders of magnitude in the gap between the average and the median of the infidelity $\bar{I}(|\psi\rangle)$ and the average is located clearly outside of the interquartile range. In contrast, the case of perfectly pure states shows that average and median have the same order of magnitude and are within the interquartile range [see Fig. 2(a)]. This indicates a large increase in the variability of the estimation accuracy of the 5BB-QT method when the unknown pure states are affected by white noise. The stagnation of the method can be explained as the result of error sources

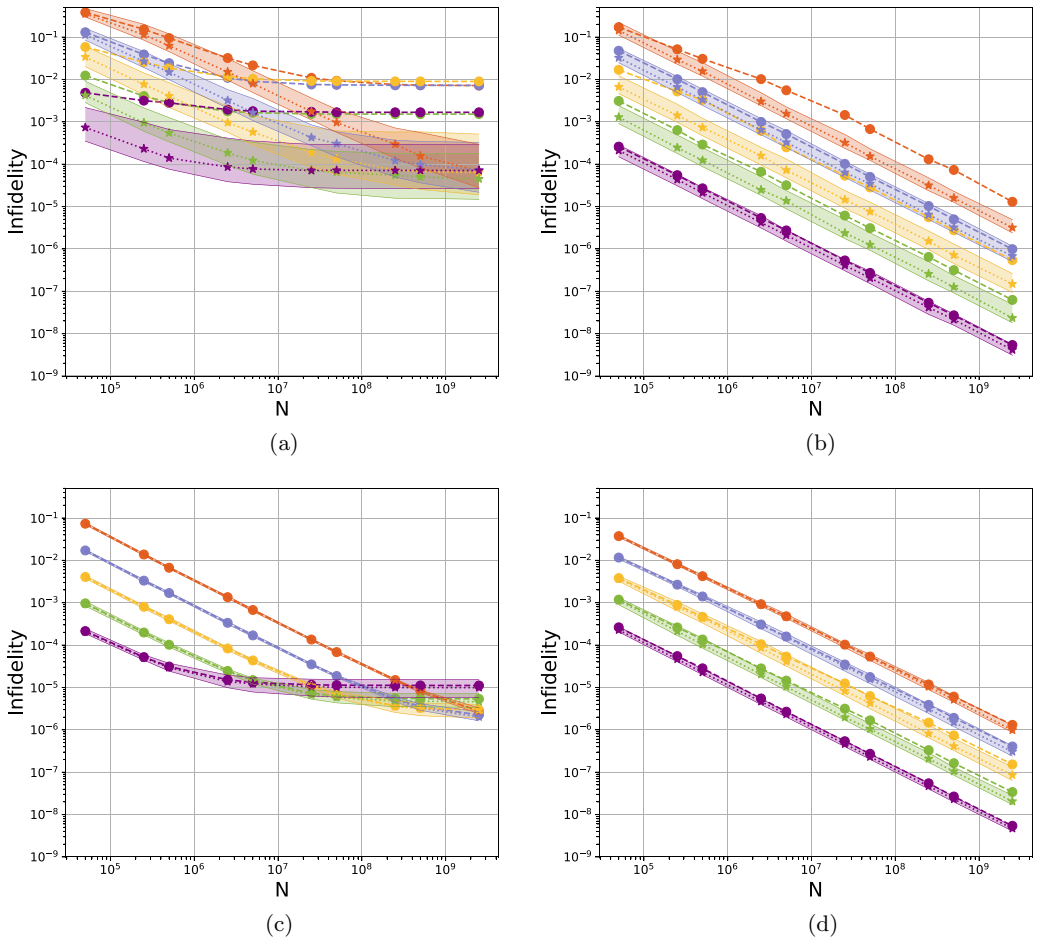

FIG. 4. Mean (solid dots) and median (solid stars) of $\bar{I}$ on states in Ω_d as a function of the ensemble size N under white noise of Eq. (17) with purity of 0.98, for dimension $d = 4$ (purple), 8 (green), 16 (yellow), 32 (blue), and 64 (red), obtained by means of the four different estimation methods: (a) 5BB-QT method, (b) C5BB-QT method, (c) I5BB-QT method, and (d) CI5BB-QT method. Shaded areas represent interquartile range.

that behave differently with respect to the ensemble size. In the case free of white noise, the only error source is the finite character of the ensemble size, which introduces an error in the estimation of the probabilities required to estimate the unknown state. As the ensemble size increases, the finite statistics effects become less severe and the estimation accuracy increases. In the limit case of an infinite ensemble size, the 5BB-QT method delivers an estimate that agrees with the unknown state. The error introduced by the white noise behaves differently. It cannot be decreased by increasing the ensemble size, as Eq. (26) shows. Thus, an increase in the ensemble size leads to an increase in the accuracy up to a certain point where the white noise becomes the dominating error source. Beyond this point, estimation accuracy cannot be increased.

The performance of the 5BB-QT method in the presence of white noise can be greatly improved. This is done by noting that the measurement results allows us to estimate the value of the unknown parameter λ. Let us consider the following two measured probabilities from the basis $\mathcal{B}_0$:

$$p'_k = (1-\lambda)|c_k|^2 + \frac{\lambda}{d}, \tag{27}$$

$$p'_{k+1} = (1-\lambda)|c_{k+1}|^2 + \frac{\lambda}{d}, \tag{28}$$

with k arbitrary. Recalling that $\Lambda'_k = 2c'_k c'^*_{k+1} = 2(1-\lambda)c_k c^*_{k+1}$, we have that

$$|\Lambda'_k|^2 = 4(1-\lambda)^2|c_0|^2|c_1|^2. \tag{29}$$

The value of Λ'_k is obtained from the bases $\mathcal{B}_i$ with $i = 1, \ldots, 4$. Solving Eqs. (27) and (28) for $|c_k|^2$ and $|c_{k+1}|^2$, respectively, and replacing in Eq. (29) we obtain

$$|\Lambda'_k|^2 = 4\left(p'_k - \frac{\lambda}{d}\right)\left(p'_{k+1} - \frac{\lambda}{d}\right). \tag{30}$$

The previous expression becomes a quadratic equation for the parameter λ, that is,

$$\frac{\lambda^2}{d^2} - \frac{\lambda}{d}(p'_k + p'_{k+1}) + p'_k p'_{k+1} - \frac{|\Lambda'_k|^2}{4} = 0. \tag{31}$$

The solution of this equation is given by

$$\lambda_k = \frac{d}{2}[p'_k + p'_{k+1} - \sqrt{(p'_k - p'_{k+1})^2 + |\Lambda'_k|^2}], \tag{32}$$

where we chose the solution with negative sign since λ must be a small quantity. Let us note that in the case of a pure state, that is, $\lambda = 0$, Eq. (32) becomes $|\Lambda'_k|^2 = 4p'_k p'_{k+1}$. This shows that the tomographic method allows one to test the purity

assumption [28]. If the experimentally acquired data originate in a mixed state, the previous condition cannot be satisfied. The estimation of λ can be carried out with any value of k and will lead to the same result $\lambda_k = \lambda$. However, due to statistical fluctuations, we propose to estimate λ as the average of the $\{\lambda_k\}$, that is,

$$\lambda = \frac{1}{d}\sum_{k=1}^{d}\lambda_k. \tag{33}$$

This choice increases the robustness of the method. Thereafter, the value of λ can be employed to correct the coefficients c'_k. The corrected coefficients c''_k are given by

$$c''_k = \sqrt{\frac{p'_k - \lambda/d}{1-\lambda}}\frac{c'_k}{|c'_k|}, \tag{34}$$

while the final estimate of $|\psi\rangle$ is

$$|\psi''\rangle = \sum_k c''_k|k\rangle. \tag{35}$$

The effect of this estimate on the C5BB-QT method is displayed in Fig. 4(b). Clearly, there is a large improvement in the estimation accuracy when compared to the case of the 5BB-QT method. The lineal behavior with respect to the ensemble size is restored, there are no signs of stagnation, the average and the median of $\bar{I}(|\psi_i\rangle)$ on Ω_d are similar, and the interquartile range is narrow. In fact, the achieved estimation accuracy resembles very much the case of the C5BB-QT method without white noise, which is displayed in Fig. 2(b). We stress the fact that this good result is achieved by noting that the projections onto the five bases $\mathcal{B}_i$ allow us to obtain the value of λ. This allows one to correct the action of the white noise onto the probabilities, Eq. (19), employed to estimate the unknown state. Furthermore, it is not necessary to increase the total number of measurement outcomes.

The effect of white noise on the I5BB-QT method is illustrated in Fig. 4(c), which depicts a different scenario for the same amount of purity as in Figs. 4(a) and 4(b). Average and median of $\bar{I}(|\psi_i\rangle)$ on Ω_d are nearly indistinguishable and the interquartile range is of the same order of magnitude as the average. The first three values of ensemble size N exhibit values of $\langle\bar{I}\rangle$ that are nearly identical to those in Fig. 2(c). Thereby, in this range of ensemble size the I5BB-QT method seems to be unaffected by the presence of noise. As the ensemble size increases, the average infidelity $\langle\bar{I}\rangle$ for the lowest dimensions enters into an asymptotic regime, as in the case of the 5BB-QT method in Fig. 4(a). Nevertheless, the loss of accuracy of the I5BB-QT method is less severe than in the case of the 5BB-QT method. Let us recall that the I5BB-QT method does not employ the probability amplitudes obtained via projections onto the base $\mathcal{B}_0$.

The results obtained by the C5BB-QT and I5BB-QT methods suggest that the CI5BB-QT method might achieve a good performance. Indeed, the best estimation accuracy is achieved by the CI5BB-QT method, as illustrated in Fig. 4(d). The lineal behavior is recovered and stagnation does not arise. The average and the median of $\bar{I}(|\psi_i\rangle)$ on Ω_d have very close values that are contained within a very narrow interquartile. The hallmark of the CI5BB-QT method is that it achieves an estimation accuracy in the presence of white noise that is almost the same as in the case without white noise depicted in Fig. 2(d). This shows that the CI5BB-QT method can reliably estimate with a high accuracy pure states affected by white noise. As in the case of the CI5BB-QT method in the absence of white noise, we can obtain an approximate expression for the mean infidelity in the presence of white noise. This approximation is given by

$$\bar{I}(|\psi_i\rangle) \approx \alpha\frac{d^{1.86}}{N^{0.97}}, \tag{36}$$

for all $|\psi_i\rangle$ in Ω_d, where the values of $\bar{\alpha}$, $\bar{\beta}$, and $\bar{\gamma}$ as functions of the dimension and the ensemble size are indicated in Table II. Thereby, the estimation accuracy achieved by the CI5BB-QT method surpasses the estimation accuracy of any tomographic method designed to estimate unknown mixed states via separable measurements.

TABLE II. Mean values and standard deviations of the coefficients α, β, and γ entering in the lineal fit of the mean infidelity, Eq. (14), generated by the CI5BB-QT method in the presence of white noise at a purity level of 0.98.

d	$\bar{\alpha}\pm\Delta_\alpha$	$\bar{\beta}\pm\Delta_\beta$	N	$\bar{\gamma}\pm\Delta_\gamma$
4	1.4 ± 0.1	1.00 ± 0.02	10^7	1.9 ± 0.2
8	0.98 ± 0.04	0.99 ± 0.05	5×10^6	1.9 ± 0.2
16	1.0 ± 0.1	0.96 ± 0.07	10^6	1.9 ± 0.1
32	1.23 ± 0.07	0.95 ± 0.05	5×10^5	1.9 ± 0.1
64	1.50 ± 0.08	0.95 ± 0.04	10^5	1.8 ± 0.1
			5×10^4	1.8 ± 0.1

The tomographic schemes here studied are based on the projection of the unknown state onto a set of bases. Another error model arises naturally by assuming that the experimental setup cannot project onto the states of the bases but onto very close states. Let us assume that $|\phi\rangle$ is one of the states of the five bases. Then, the experimental setup implements a projection onto the state

$$|\tilde{\phi}\rangle = \frac{|\phi\rangle + c|\eta\rangle}{\sqrt{1+2c\mathrm{Re}(\langle\phi|\eta\rangle)+c^2}}, \tag{37}$$

where c is a non-negative constant and the state $|\eta\rangle$ is chosen uniformly in the corresponding Hilbert space. The normalization constant takes account of the nonorthogonality between $|\phi\rangle$ and $|\eta\rangle$.

The probability of projecting the unknown state $|\psi\rangle$ onto $|\tilde{\phi}\rangle$ is given by the expression

$$|\langle\psi|\tilde{\phi}\rangle|^2 = \frac{|\langle\psi|\phi\rangle|^2 + 2c\mathrm{Re}(\langle\phi|\psi\rangle\langle\phi|\eta\rangle) + c^2|\langle\psi|\eta\rangle|^2}{1+2c\mathrm{Re}(\langle\phi|\eta\rangle)+c^2}. \tag{38}$$

Since the states $|\eta\rangle$ are randomly chosen, we calculate the average of $|\langle\psi|\tilde{\phi}\rangle|^2$, that is,

$$\int d\eta|\langle\psi|\tilde{\phi}\rangle|^2 = \frac{1}{1+c^2}|\langle\psi|\phi\rangle|^2 + \frac{c^2}{1+c^2}\frac{1}{d}, \tag{39}$$

where we have employed the properties $\int d\eta|\eta\rangle = 0$ and $\int d\eta|\eta\rangle\langle\eta| = (1/d)I$ of the Haar measure $d\eta$ on the Hilbert

space of dimension d. With the identification $\lambda = c^2/(1 + c^2)$, the previous expression becomes identical to the white-noise model of Eq. (19). Therefore, both error models—white noise and approximate projections—are identical, as long as λ and c are constant.

VII. DISCUSSION AND CONCLUSIONS

We have studied the accuracy achieved in the process of estimating pure quantum states of finite-dimensional quantum systems. We have resorted to the 5BB-QT method, which was specifically designed to reconstruct pure states. This method is based on the projection of the unknown state onto five different bases regardless of the dimension of the system. Also, the method does not require the use of postprocessing and can certify whether the data originate from a pure state or not. As figure of merit for the estimation accuracy we employ the mean infidelity $\bar{I}(|\psi\rangle)$, that is, the infidelity averaged over a large set of estimates for a fixed unknown state $|\psi\rangle$. The 5BB-QT method is characterized by a state dependent accuracy, where the mean infidelity $\bar{I}(|\psi\rangle)$ can fluctuate two orders of magnitude. In fact, average and median of $\bar{I}(|\psi\rangle)$ over Ω_d lead to values that can differ by one order of magnitude, which reveals the variability of the estimation accuracy provided by the 5BB-QT method. The average $\langle\bar{I}\rangle$ as a function of ensemble size N exhibits a linear behavior that resembles the Gill-Massar lower bound $I_{\mathrm{GM}}^{(\mathrm{mixed})}$.

The 5BB-QT method employs a recursive relation to estimate the absolute value and the phase of the probability amplitudes that define a pure state. This recursion is such that small probability amplitudes lead to a poor estimation of the absolute values and the phases, which in turn lead to a decrease in the estimation accuracy of the method. In order to improve the estimation accuracy of the 5BB-QT method we have proposed three modifications for the estimation procedure employed by the 5BB-QT method, each one of them reaching a higher accuracy. Instead of estimating the absolute value of the probability amplitudes via the recursive equation system, we can simply employ the information obtained by the projections onto the base $\mathcal{B}_0$. This allows for an independent estimate of each absolute value, which increases the accuracy. The information provided by the base $\mathcal{B}_0$ can also be employed to increase the estimation of the complex phases by ordering the absolute values of the probability amplitudes in decreasing order and solving thereafter the recursive equations system. These two modifications of the estimation procedure lead to the CI5BB-QT method, which exhibits a significant increase in the estimation accuracy. The estimation accuracy provided by the CI5BB-QT method exhibits an average over the set of pure states that is indistinguishable from the median, both being central tendency indicators contained in a very narrow interquartile range. This is an indication of a state independent accuracy. In fact, the estimation accuracy of the CI5BB-QT method can be approximated by the expression $\bar{I}(|\psi\rangle) = \alpha d^{1.87}/N$. Thus, the CI5BB-QT method provides an accuracy that is at least one order of magnitude higher than the one provided by the 5BB-QT method. Furthermore, the CI5BB-QT method surpasses the Gill-Massar lower bound $I_{\mathrm{GM}}^{(\mathrm{mixed})}$ for the estimation accuracy of unknown mixed states, which behaves asymptotically as $O(d^3/N)$.

We have also studied the accuracy achieved in the process of estimating pure quantum states in the presence of a small level of white noise, which transforms pure states into mixed ones. In this case, the 5BB-QT method exhibits a severe loss of accuracy and stagnation; that is, after a certain value of ensemble size the estimation accuracy becomes constant and cannot be improved by a further increase in N. At a purity of 0.98, the average $\langle\bar{I}\rangle$ generated by the 5BB-QT method enters into stagnation for an ensemble size of approximately 10^7. In this regime, the infidelity stays within the interval $[10^{-3}, 10^{-2}]$, independently of the dimension. This represents, for some dimensions, a dramatic increase in the infidelity by two orders of magnitude, when compared to the noiseless case. The median also shows signs of stagnation reaching values in the interval $[10^{-5}, 10^{-4}]$, albeit for a higher value of $N \approx 10^9$. The gap between the average and the median of $\bar{I}(|\psi\rangle)$ also increases in such a way that the average is several orders of magnitude beyond the interquartile range. This indicates an increase in the variability of the estimation accuracy. Thus, a purity of 0.98 severely decreases the estimation accuracy of the 5BB-QT method. The CI5BB-QT method behaves differently. We have shown that the information provided by the projections onto the base $\mathcal{B}_0$ allows one to correct the errors introduced by the white noise. This correction leads to an estimation accuracy for the CI5BB-QT method that resembles very closely the one achieved in the absence of white noise. In the presence of white noise generating a purity of 0.98, the CI5BB-QT method achieves an estimation accuracy that can be approximated as $\bar{I}(|\psi\rangle) = \alpha d^{1.86}/N^{0.97}$. This also surpasses the Gill-Massar lower bound $I_{\mathrm{GM}}^{(\mathrm{mixed})}$ in the inspected ranges of dimension and ensemble size.

The 5BB-QT method was experimentally realized in dimension $d = 8$ by means of a single spatial qudit. This is generated by discretizing the transverse momentum of a single photon with the help of diffractive optical elements, such as physical slits [42] or spatial light modulators [9]. The 5BB-QT and CI5BB-QT methods employ the same number and type of measurements. Thereby, spatial qudits are a feasible scenario for the implementation of the CI5BB-QT method in higher dimensions. Recently, in a comparative study among various tomographic methods [43], the 5BB-QT method was implemented in dimension $d = 16$ by means of the coupled electron-nuclear spins of individual ^{133}Cs atoms in the electronic ground state. This is also a feasible test bed for the CI5BB-QT method.

Finally, we would like to comment on a peculiarity of the 5BB-QT method and of its variations. These allow one to determine whether the experimentally acquire data originate in a pure state or a mixed one; that is, it is possible to test the purity assumption. This is done by testing the conditions $|\Lambda'_k|^2 = 4p'_k p'_{k+1}$ for $k = 0, \ldots, d-1$. This is possible whenever we have an infinite ensemble size. If this is not the case, it is possible to conceive the existence of a variety of mixed states that, within the inaccuracy of the inferred probabilities, exhibit the same statistics of the estimate provided by the 5BB-QT method or its variations. This leads naturally to the question of the existence and characterization of mixed estimates that are closer to the unknown pure state than the pure estimate [44]. From the numerical point of view, we can resort to maximum likelihood estimation on the space of mixed states.

Since the set of five bases lacks informational completeness at the level of the full set of density matrices, the solution will not be unique. Within the set of solutions we can search for the mixed state which minimizes the infidelity with respect to the unknown state. An alternative approach is the use of the the so-called physical imposition operator [45], which constructs states with predefined statistics. These two methods might allow us to study the question of the existence of more accurate mixed estimates that are close to the unknown state. However, these approaches fail to provide a mixed estimate, since they require knowledge about the state to be determined. We can, however, study this problem in a reduced set of density matrices. As we have shown in the previous section, the CI5BB-QT method can deliver an estimate $|\tilde{\psi}\rangle$ for a pure state $|\psi\rangle$ that is transformed into the mixed state $\rho = (1-\lambda)|\psi\rangle\langle\psi| + (\lambda/d)I$ by the action of white noise. Equivalently, we can construct an estimate for ρ given by $\tilde{\rho} = (1-\tilde{\lambda})|\tilde{\psi}\rangle\langle\tilde{\psi}| + (\tilde{\lambda}/d)I$. The infidelity of $\tilde{\rho}$ with respect to $|\psi\rangle$ is given by $\langle\psi|\tilde{\rho}|\psi\rangle = (1-\lambda)|\langle\psi|\tilde{\psi}\rangle|^2 + (\lambda/d)$, where we have assumed that λ and its estimate $\tilde{\lambda}$ are very close. This infidelity will be smaller than the infidelity of $|\psi\rangle$ with respect to $|\tilde{\psi}\rangle$ whenever $1-|\langle\psi|\tilde{\psi}\rangle|^2 > (d-1)/d$. However, for moderate ensemble sizes, the CI5BB-QT method already delivers infidelities $1-|\langle\psi|\tilde{\psi}\rangle|^2$ which are much smaller than $(d-1)/d$. Consequently, the estimate $\tilde{\rho}$ can be ruled out in the case of a larger ensemble size. This is an interesting problem that deserves independent study.

In summary, the estimation procedure of the 5BB-QT method can be suitably modified to achieve a higher estimation accuracy, which surpasses the estimation accuracy of any tomographic method designed to estimate unknown mixed states. This method, the CI5BB-QT method, preserves the estimation accuracy even in the presence of a small level of white noise in a wide range of dimensions and ensemble sizes, with the added benefit of a total number of projective measurements that scales linearly with the dimension. Experimental realizations of the CI5BB-QT method in high dimensions are well within reach of today's experimental setups.

ACKNOWLEDGMENTS

This work was funded by the Millennium Institute for Research in Optics and by CONICYT FONDECYT Grant No. 1180558. L.Z. was supported by CONICYT-PCHA Doctorado Nacional Grant No. 2017-21181021.

[1] D. F. V. James, P. G. Kwiat, W. J. Munro, and A. G. White, Phys. Rev. A **64**, 052312 (2001).
[2] R. T. Thew, K. Nemoto, A. G. White, and W. J. Munro, Phys. Rev. A **66**, 012303 (2002).
[3] J. Schwinger, Proc. Natl. Acad. Sci. USA **46**, 570 (1960).
[4] I. D. Ivanovic, J. Phys. A **14**, 3241 (1981).
[5] W. K. Wootters and B. D. Fields, Ann. Phys. (NY) **191**, 363 (1989).
[6] A. B. Klimov, C. Muñoz, A. Fernández, and C. Saavedra, Phys. Rev. A **77**, 060303(R) (2008).
[7] S. N. Filippov and V. I. Man'ko, Phys. Scr. **T143**, 14010 (2011).
[8] R. B. A. Adamson and A. M. Steinberg, Phys. Rev. Lett. **105**, 030406 (2010).
[9] G. Lima, L. Neves, R. Guzman, E. S. Gomez, W. A. T. Nogueira, A. Delgado, A. Vargas, and C. Saavedra, Opt. Exp. **19**, 3542 (2011).
[10] E. Prugovečki, Int. J. Theor. Phys. **16**, 321 (1977).
[11] J. M. Renes, R. Blume-Kohout, A. J. Scott, and C. M. Caves, J. Math. Phys. **45**, 2171 (2004).
[12] T. Durt, C. Kurtsiefer, A. Lamas-Linares, and A. Ling, Phys. Rev. A **78**, 042338 (2008).
[13] Z. E. D. Medendorp, F. A. Torres-Ruiz, L. K. Shalm, G. N. M. Tabia, C. A. Fuchs, and A. M. Steinberg, Phys. Rev. A **83**, 051801(R) (2011).
[14] N. Bent, H. Qassim, A. A. Tahir, D. Sych, G. Leuchs, L. L. Sanchez-Soto, E. Karimi, and R. W. Boyd, Phys. Rev. X **5**, 041006 (2015).
[15] W. M. Pimenta, B. Marques, T. O. Maciel, R. O. Vianna, A. Delgado, C. Saavedra, and S. Padua, Phys. Rev. A **88**, 012112 (2013).
[16] R. Salazar and A. Delgado, Phys. Rev. A **86**, 012118 (2012).
[17] C. Paiva-Sanchez, E. Burgos-Inostroza, O. Jiménez, and A. Delgado, Phys. Rev. A **82**, 032115 (2010).
[18] D. Martínez, M. A. Solís-Prosser, G. Cañas, O. Jiménez, A. Delgado, and G. Lima, Phys. Rev. A **99**, 012336 (2019).
[19] Q. Pears Stefano, L. Rebón, S. Ledesma, and C. Iemmi, Phys. Rev. A **96**, 062328 (2017).
[20] Q. Pears Stefano, L. Rebón, S. Ledesma, and C. Iemmi, Opt. Lett. **44**, 2558 (2019).
[21] D. Ahn, Y. S. Teo, H. Jeong, F. Bouchard, F. Hufnagel, E. Karimi, D. Koutný, J. Řeháček, Z. Hradil, G. Leuchs, and L. L. Sánchez-Soto, Phys. Rev. Lett. **122**, 100404 (2019).
[22] Z. Hradil, Phys. Rev. A **55**, R1561 (1997).
[23] S. M. Tan, J. Mod. Opt. **44**, 2233 (1997).
[24] M. S. Kaznady and D. F. V. James, Phys. Rev. A **79**, 022109 (2009).
[25] R. Blume-Kohout, New J. Phys. **12**, 043034 (2010).
[26] H. Häffner, W. Hänsel, C. F. Roos, J. Benhelm, D. Chek-al-kar, M. Chwalla, T. Körber, U. D. Rapol, M. Riebe, P. O. Schmidt, C. Becher, O. Gühne, W. Dür, and R. Blatt, Nature (London) **438**, 643 (2005).
[27] S. T. Flammia, A. Silberfarb, and C. Caves, Found. Phys. **35**, 1985 (2005).
[28] D. Goyeneche, G. Cañas, S. Etcheverry, E. S. Gómez, G. B. Xavier, G. Lima, and A. Delgado, Phys. Rev. Lett. **115**, 090401 (2015).
[29] D. Gross, Y. K. Liu, S. T. Flammia, S. Becker, and J. Eisert, Phys. Rev. Lett. **105**, 150401 (2010).
[30] C. H. Baldwin, I. H. Deutsch, and A. Kalev, Phys. Rev. A **93**, 052105 (2016).
[31] N. Li, C. Ferrie, J. A. Gross, A. Kalev, and C. M. Caves, Phys. Rev. Lett. **116**, 180402 (2016).

[32] M. Cramer, M. B. Plenio, S. T. Flammia, R. Somma, D. Gross, S. D. Bartlett, O. Landon-Cardinal, D. Poulin, and Y.-K. Liu, Nat. Commun. **1**, 149 (2010).
[33] D. H. Mahler, L. A. Rozema, A. Darabi, C. Ferrie, R. Blume-Kohout, and A. M. Steinberg, Phys. Rev. Lett. **111**, 183601 (2013).
[34] L. Pereira, L. Zambrano, J. Cortés-Vega, S. Niklitschek, and A. Delgado, Phys. Rev. A **98**, 012339 (2018).
[35] G. I. Struchalin, E. V. Kovlakov, S. S. Straupe, and S. P. Kulik, Phys. Rev. A **98**, 032330 (2018).
[36] Z. Hou, H. Zhu, G. Xiang, C.-F. Li, and G.-C. Guo, Npj Quantum Inf. **2**, 16001 (2016).
[37] M. G. A. Paris, Int. J. Quantum. Inform. **07**, 125 (2009).
[38] R. D. Gill and S. Massar, Phys. Rev. A **61**, 042312 (2000).
[39] H. Zhu and M. Hayashi, Phys. Rev. Lett. **120**, 030404 (2018).
[40] R. Jozsa, J. Mod. Opt. **41**, 2315 (1994).
[41] M. Hübner, Phys. Lett. A **163**, 239 (1992).
[42] L. Neves, G. Lima, J. G. Aguirre Gómez, C. H. Monken, C. Saavedra, and S. Padua, Phys. Rev. Lett. **94**, 100501 (2005).
[43] H. Sosa-Martinez, N. K. Lysne, C. H. Baldwin, A. Kalev, I. H. Deutsch, and P. S. Jessen, Phys. Rev. Lett. **119**, 150401 (2017).
[44] We would like to acknowledge the anonymous referee for pointing out this problem.
[45] D. M. Goyeneche and A. C. de la Torre, Phys. Rev. A **77**, 042116 (2008).